



Backbone NMR Assignments of a Putative p53-binding Domain of the Mitochondrial Hsp40, Tid1

Ku-Sung Jo¹, Dae-Won Sim¹, Eun-Hee Kim², Dong-Hoon Kang³, Yu-Bin Ma³, Ji-Hun Kim^{3,*} and Hyung-Sik Won^{1,*}

¹Department of Biotechnology, College of Biomedical and Health Science, Konkuk University, Chungju, Chungbuk 27478, Korea

²Protein Structure Group, Korea Basic Science Institute, Ochang, Chungbuk 28119, Korea

³College of Pharmacy, Chungbuk National University, Cheongju, Chungbuk 28160, Korea

Received Aug 20, 2018; Revised Sep 3, 2018; Accepted Sep 10, 2018

Abstract Human Tid1, belonging to the family of the Hsp40/DnaJ, functions as a co-chaperone of cytosolic and mitochondrial Hsp70 proteins. In addition, the conserved J-domain and G/F-rich region of Tid1 has been suggested to interact with the p53 tumor suppressor protein, to translocate it to the mitochondria. Here, backbone NMR assignments were achieved for the putative p53-binding domain of Tid1. The obtained chemical shift information identified five α -helices including four helices characteristic of J-domain, which are connected to a short α -helix in the G/F-rich region via a flexible loop region. We expect that this structural information would contribute to our progressing studies to elucidate atomic structure and molecular interaction of the domain with p53.

Keywords Tid1, mitochondria, Hsp40, J domain, G/F-rich region, p53-binding domain

Introduction

Molecular chaperones play vital roles in protein regulation by assisting in several key cellular functions, such as folding process of both nascent and damaged proteins, translocation of proteins into

their proper cellular spots, and suppression of protein aggregation.^{1,2} Heat shock proteins (Hsps) represent the most well-known group of molecular chaperones of which expression is induced by heat and other stresses.³ Among them, a specific chaperon pair of Hsp70 and Hsp40 is also known to play important roles in a range of cellular events.^{4,5} Hsp40 and its homologous proteins recruit polypeptide substrates to Hsp70 and bind directly to Hsp70. Their direct binding stimulates both the substrate interaction with Hsp70 and otherwise weak activity of its ATP hydrolysis.⁶ In *Escherichia coli*, DnaJ and DnaK are well-characterized as bacterial counterparts of Hsp40 and Hsp70, respectively.

The Hsp40/DnaJ-family possess very diverse primary sequences but generally share four typical domains in various combinations: a highly conserved N-terminal J-domain (JD), a glycine/phenylalanine (G/F)-rich region, a cysteine repeat (Cys-repeat) region containing zinc-finger motifs, and a less well conserved C-terminal substrate-binding domain.⁷ For example, Type-I DnaJ (DnaJA, 4 members) consists of all four domains, whereas type-II DnaJ (DnaJB, 13 members) lacks the Cys-repeat region, and type-III DnaJ (DnaJC, 32 members) lacks both the G/F-rich and Cys-repeat regions.⁷⁻⁹ In this respect, JD of Hsp40/DnaJ can be considered as a principle region

*Correspondence to: **Hyung-Sik Won**, Department of Biotechnology, College of Biomedical and Health Science, Konkuk University, Chungju, Chungbuk 27478, Korea, Tel: 82-43-840-3589, E-mail: wonhs@konkuk.ac.kr

that represents the functional unique property. JD is a small protein domain usually consisting of about 70 amino acids, and is known to control ATPase activity of Hsp70 by the cis-interaction between a highly

conserved tripeptide HPD (histidine, proline and aspartic acid) motif in the JD and the ATPase domain of Hsp70.¹⁰⁻¹²

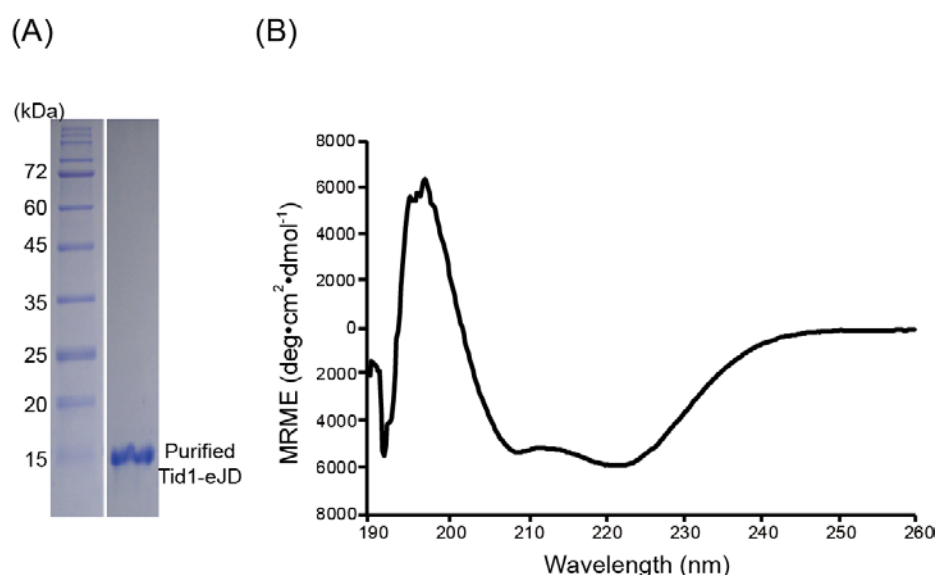


Figure 1. Purification and structural characterization of the recombinant Tid1-eJD. (A) Purified Tid1-eJD in SDS-PAGE. (B) Far-UV CD spectrum of the purified Tid1-eJD.

Human Tid1 (tumorous imaginal disc protein 1), encoded by *DnaJA3* gene, is a mitochondrial Hsp40 (mtHsp40) having the N-terminal mitochondria-targeting sequence (residues 1-65) that is cleaved upon its mitochondrial localization. After translocation to the mitochondria, Tid1 is expected to function primarily as a co-chaperone of mtHsp70 (also called mortalin) for initiation of the mitochondrial Hsp70-Hsp40 chaperone system.¹³⁻¹⁵ In addition, Tid1 has also been suggested to translocate the p53 tumor suppressor protein to the mitochondria, which triggers the mitochondrial apoptosis progress by p53.¹⁶ In this machinery process, G/F-rich region (residues 158-201) of Tid1 has also appeared to be involved in the p53 interaction, although the JD (residues 91-158) was suggested as a minimal and essential unit for the interaction.^{10, 17, 18} Considering p53 as a known client of mortalin, it is presumable that the JD and

G/F-rich region of Tid1 would be responsible for the possible regulation of both p53 and mortalin.

In this context, we aimed to achieve backbone NMR assignments of the putative p53-binding domain (JD + G/F-rich region) of Tid1, for preliminary structural characterization of the domain.

Experimental Methods

Protein preparation – The cDNA of Tid1 was amplified by polymerase chain reaction (PCR) in the region corresponding to residues 89 to 192 (named herein extended JD, eJD) of Tid1, followed by insertion into a pColdI (Takara) vector, using two restriction endonuclease sites, *NdeI* and *XhoI*. Stable isotope ¹⁵N- and ¹³C/¹⁵N-enrichments of recombinant Tid1-eJD were performed as described previously.¹⁹ Proteins were overexpressed in *Escherichia coli*

BL21(DE3)pLysS strain transformed with the constructed plasmid, followed by purification via sequential application of a nickel-affinity (HisTrap FF, GE Healthcare) and a gel-filtration (HiLoad 16/60 Superdex 75, Pharmacia) column chromatography. The tagged N-terminal histidines

were then cleaved with the protease, factor Xa, followed by the removal of factor Xa and other impurities via the final gel-filtration step for buffer-exchange.

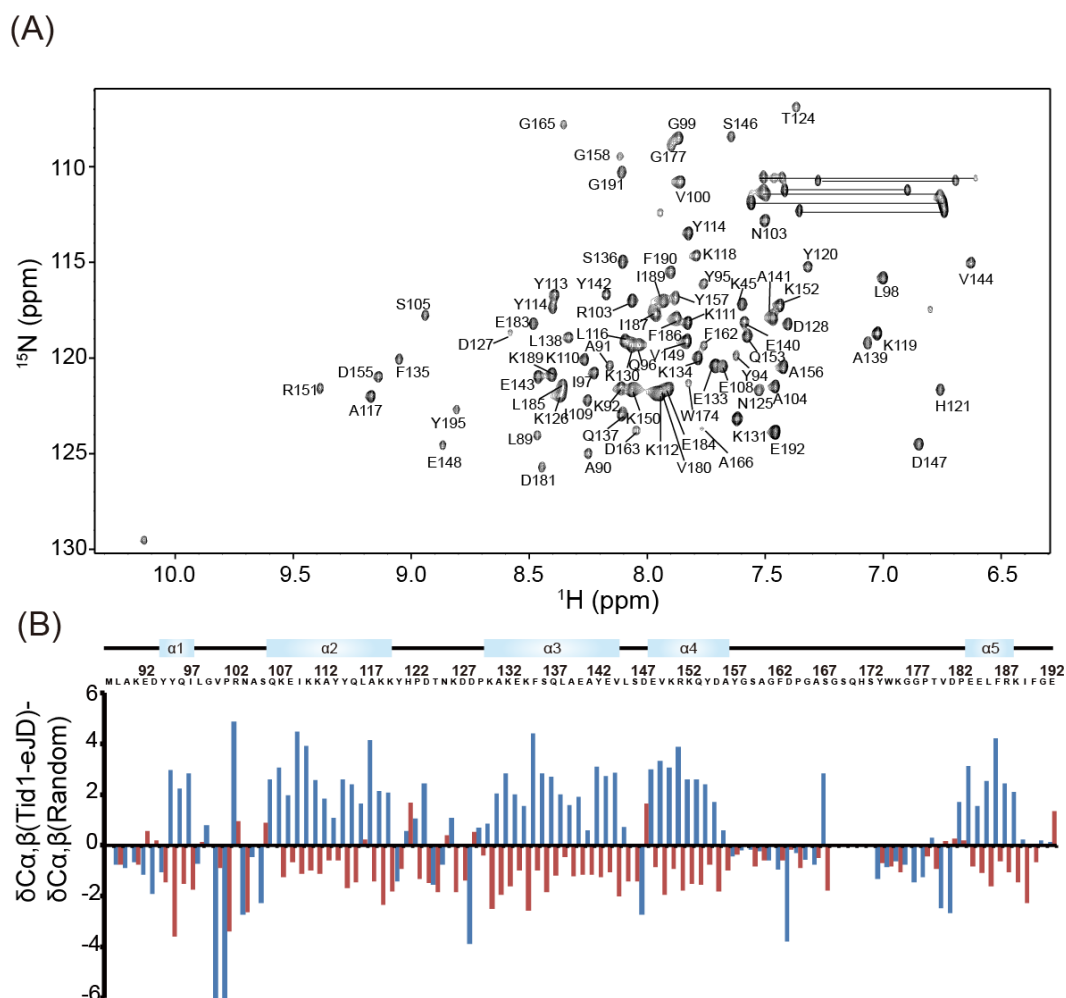


Figure 2. NMR assignments and secondary structure determination. (A) 2D- $[^1\text{H}/^{15}\text{N}]$ HSQC spectrum of Tid1-eJD labeled with sequence-specific assignments of individual resonances. Resonances paired with lines originated from side chains of Gln or Asn. (B) CSI-based secondary structure determination. $^{13}\text{C}\alpha$ (blue) and $^{13}\text{C}\beta$ (red) chemical shift deviations from reference values (random-coil chemical shifts) are plotted along the amino acid sequence. Determined secondary structure elements are shown over the sequence line.

CD (Circular Dichroism) Spectroscopy – A standard far-UV CD spectrum of 16 μM Tid1-eJD dissolved in 20 mM Tris-HCl buffer (pH 7.0) was measured at

room temperature (approximately 22 $^\circ\text{C}$) on a Jasco J-715 Spectrometer (Applied Photophysics, UK). Three individual scans taken from 260 to 190 nm

were summed and averaged, followed by subtraction of solvent CD signals. Finally, the CD intensity was normalized as the mean residue molar ellipticity (MRME).²⁰

acquired using Bruker Biospin Avance 800 MHz spectrometer equipped with a cryoprobe, at KBSI (Korea Basic Science Institute, Ochang, Korea). 2D- $^1\text{H}/^{15}\text{N}$ HSQC spectra were measured with 0.3 mM of

NMR experiments and analysis – NMR spectra were

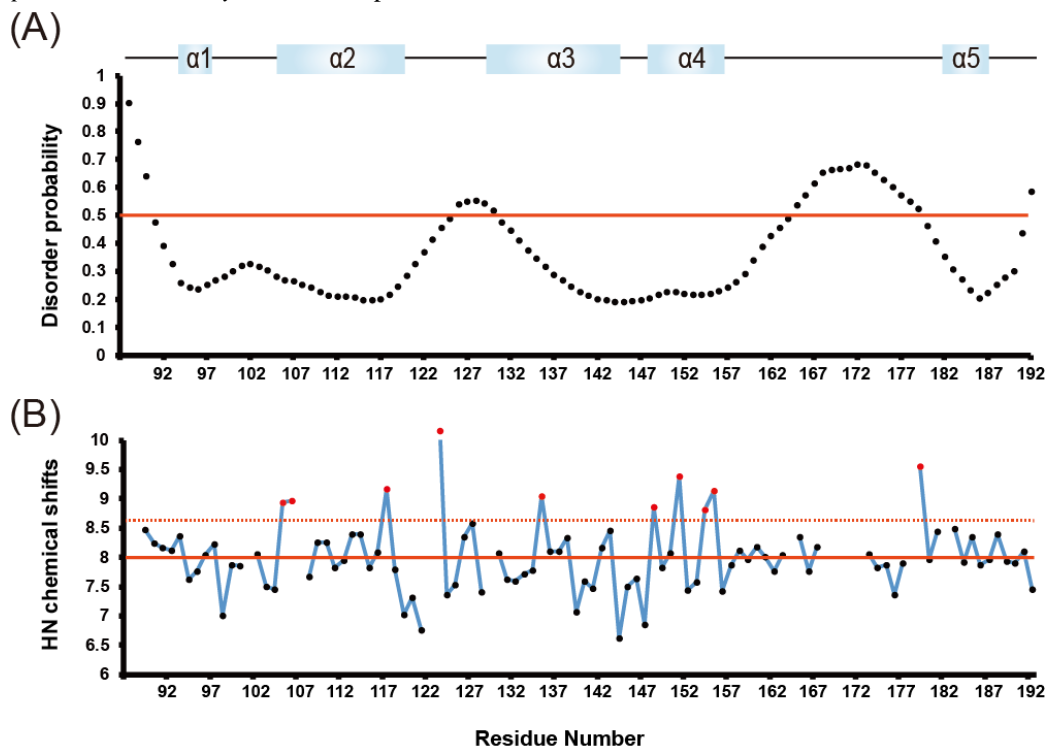


Figure 3. Structural characterization of Tid1-eJD based on amino acid sequence and backbone amide chemical shift values, using disorder region prediction and chemical shift analysis. (A) Disorder probability plot. Residues beyond the threshold (red line) are predicted to be disordered. (B) Assigned δHN plot. Red dots indicate the residues with a prominent down-field shift beyond the standard deviation (red dotted line) from mean value (red solid line).

^{15}N Tid1-eJD dissolved in a 20 mM Tris-HCl buffer containing 300 mM NaCl, 1 mM dithiothreitol, and 7% D_2O . The sequential backbone resonance assignments of $[\text{U-}^{13}\text{C}/^{15}\text{N}]$ Tid1-eJD were carried out using HSQC-based triple resonance experiments, including HNCACB, CBCA(CO)NH, HNCO and HN(CA)CO pulse sequences. NMR data were processed using NMRPipe²¹ and analyzed using NMRView. The assigned $\text{C}\alpha$ and $\text{C}\beta$ chemical shifts of Tid1-eJD were used for secondary structure determination, on the basis of the chemical shift index (CSI) method.²²

Results and Discussion

Preparation and characterization of recombinant protein – Our initial attempt to prepare the recombinant protein corresponding to the region (residues 89-235) between the mitochondrial targeting sequence (residues 1-65) and Cys-rich region (residues 235-296) was not successful due to the inclusion body formation of the expressed protein (data not shown). However, the C-terminally shorter construct eJD (residues 89-192) that covers the whole region of JD (residues 91-158) and most region of G/F-rich region (residues 158-201) was successfully

over-expressed and purified (Figure 1A). After cleavage of the artificial his-tag at the N-terminus, the apparent molecular mass of the Tid1-eJD (14.5 kDa), estimated by gel-filtration, was in good agreement with its theoretical monomeric molecular weight of 12.1 kDa (data not shown). The standard

far-UV CD spectrum of Tid1-eJD, which was characterized by a positive band at 196 nm and strong negative bands with double minima near 208 and 222 nm, indicated that the protein adopted a well folded

Table 1. Chemical shift values of ^1HN , ^{15}N , $^{13}\text{C}\alpha$, $^{13}\text{C}\beta$, and ^{13}CO of Tid1-eJD.

Residue	HN	N	C α	C β	CO	Residue	HN	N	C α	C β	CO
88 M	n.d.	124.239	n.d.	30.329	n.d.	141 A	7.467	117.894	51.077	15.844	175.731
89 L	8.466	124.057	52.322	39.629	174.152	142 Y	8.172	116.663	59.676	35.44	175.201
90 A	8.248	124.989	49.603	16.556	174.691	143 E	8.462	120.98	57.34	26.852	174.74
91 K	8.159	120.416	53.54	30.343	173.567	144 V	6.628	115.01	63.057	28.884	173.04
92 E	8.11	121.579	53.457	28.438	172.768	145 L	7.506	111.341	53.827	38.971	174.733
93 D	8.366	121.983	50.274	39.289	174.064	146 S	7.644	108.433	56.229	60.392	170.567
94 Y	7.623	119.872	55.554	35.244	174.565	147 D	6.848	124.505	49.447	40.733	172.35
95 Y	7.759	116.129	59.56	33.093	175.743	148 E	8.866	124.539	57.595	27.053	175.918
96 Q	8.033	119.303	55.923	25.883	177.357	149 V	7.831	119.102	63.506	28.941	176.383
97 I	8.223	120.793	61.909	35.057	174.592	150 K	8.064	121.675	57.242	30.159	176.465
98 L	6.999	115.809	52.354	40.516	172.774	151 R	9.387	121.604	57.892	27.122	174.984
99 G	7.865	108.5	43.892	n.d.	172.626	152 K	7.437	117.246	56.785	29.591	177.442
100 V	7.86	110.805	54.102	30.006	170.201	153 Q	7.576	118.848	56.295	25.847	175.292
101 P	n.a.	117.2	55.097	26.717	174.183	154 Y	8.807	122.69	59.004	35.924	176.094
102 R	8.064	117.004	58.88	29.861	173.742	155 D	9.138	120.988	53.9	37.299	175.453
103 N	7.501	112.827	48.361	34.271	173.006	156 A	7.422	120.47	51.089	16.004	176.473
104 A	7.455	121.492	50.046	17.069	175.028	157 Y	7.879	116.831	56.16	36.337	174.515
105 S	8.94	117.774	54.036	62.687	172.572	158 G	8.116	109.459	42.886	n.a.	171.72
106 Q	8.963	119.64	56.293	n.d.	176.402	159 S	7.959	115.314	56.137	60.97	171.99
107 K	n.d.	120.609	57.244	29.849	176.618	160 A	8.173	124.65	50.269	16.41	175.423
108 E	7.678	120.446	56.56	27.248	177.045	161 G	8.01	106.563	42.486	n.a.	170.743
109 I	8.252	122.225	63.555	35.666	173.945	162 F	7.759	119.401	54.748	36.991	171.79
110 K	8.264	120.072	58.103	30.112	175.122	163 D	8.046	123.79	48.403	38.92	n.d.
111 K	7.827	118.166	56.751	29.965	175.836	164 P	n.a.	108.008	61.005	29.2	174.928
112 A	7.943	121.878	52.323	16.4	177.048	165 G	8.354	107.808	42.542	n.a.	171.666
113 Y	8.392	116.729	57.668	36.096	173.26	166 A	7.768	123.7	49.739	16.485	175.35
114 Y	8.4	117.359	59.181	35.027	174.006	167 S	8.173	114.602	59.116	60.024	175.071
115 Q	7.823	113.479	56.102	25.939	176.985	168 G	n.d.	n.d.	n.d.	n.d.	n.d.
116 L	8.094	119.098	54.747	40.615	175.311	169 S	n.d.	n.d.	n.d.	n.d.	n.d.
117 A	9.169	122.015	54.651	15.562	177.284	170 Q	n.d.	n.d.	n.d.	n.d.	n.d.
118 K	7.79	114.635	56.335	28.764	176.473	171 H	n.d.	n.d.	n.d.	n.d.	n.d.
119 K	7.024	118.713	56.269	29.282	175.169	172 S	n.d.	n.d.	n.d.	n.d.	n.d.
120 Y	7.318	115.216	55.169	35.765	170.157	173 Y	8.049	121.716	55.277	35.986	172.57
121 H	6.759	121.659	53.547	28.687	172.577	174 W	7.825	121.303	54.622	26.757	172.947
122 P	n.a.	n.d.	62.333	28.764	n.d.	175 K	7.877	124.075	53.576	30.041	173.683
123 D	11.118	121.946	54.614	37.612	175.686	176 G	7.36	108.632	42.342	n.a.	171.08
124 T	7.368	106.865	58.236	65.947	171.506	177 G	7.896	108.882	41.645	n.a.	179.543
125 N	7.526	121.685	50.348	37.285	171.86	178 P	n.a.	116.558	60.055	29.673	174.732
126 K	8.357	121.613	55.273	29.259	174.308	179 T	9.558	116.319	60.09	66.857	171.85
127 D	8.58	118.657	52.158	37.696	172.192	180 V	7.962	121.919	57.717	31.073	171.749
128 D	7.402	118.216	48.301	39.623	173.031	181 D	8.447	125.715	49.513	39.345	172.852
129 P	n.a.	119.51	61.972	29.692	176.526	182 P	n.a.	118.32	63.013	30.301	175.655
130 K	8.066	119.324	55.051	28.598	176.208	183 E	8.483	118.203	57.722	27.08	176.337
131 A	7.618	123.175	52.547	15.035	175.77	184 E	7.911	121.631	56.134	26.805	176.002
132 K	7.598	117.186	57.018	29.465	176.763	185 L	8.352	121.619	55.633	38.791	174.871
133 E	7.713	120.395	56.59	26.894	176.362	186 F	7.876	117.927	59.893	36.955	174.867
134 K	7.783	120.002	55.752	28.512	175.857	187 R	7.965	117.681	56.421	27.825	176.642
135 F	9.05	120.05	60.117	36.612	176.008	188 K	8.403	120.853	56.294	29.637	175.763
136 S	8.104	114.957	59.113	59.954	176.064	189 I	7.931	117.019	59.326	34.523	175.075
137 Q	8.107	122.95	56.383	26.194	176.064	190 F	7.899	115.515	55.629	36.936	173.961
138 L	8.333	118.933	55.114	39.924	174.645	191 G	8.108	110.285	43.288	n.a.	170.479
139 A	7.066	119.221	52.084	15.782	175.666	192 E	7.456	123.875	54.733	29.257	n.d.
140 E	7.589	118.131	56.501	26.744	174.371						

n.a., not available; n.d., not detected.

conformation with a predominant α -helical contents of secondary structure (Figure 1B).

Backbone NMR assignments – The backbone amide resonances of Tid1-eJD in the 2D- $^1\text{H}/^{15}\text{N}$ HSQC spectrum exhibited a good dispersion of resonances, supporting the well-ordered conformation (Figure 2A). Based on the 3D NMR spectra analysis, we succeeded in assigning 100 of 105 expected backbone resonances. Two peaks in the HSQC spectrum could not be assigned (Figure 2A) because the corresponding peaks were not found in the 3D spectra. Finally, backbone resonances of the five residues (residues 168-172) in the G/F-rich region were missing in the assignments (Table 1). Given that these residues didn't show up as NMR signals, the corresponding region in Tid1-eJD is supposed to adopt a disordered conformation, of which dynamic fluctuation occurs at an intermediate rate of chemical exchange in the NMR time scale.

Secondary structure of the other regions with the unambiguous assignments could be determined by the CSI-based secondary shift analysis of $^{13}\text{C}\alpha$ and $^{13}\text{C}\beta$ (Figure 2B). The result clearly identified five α -helices, four in JD and one in the extended region: helix 1, residues 8-10; helix 2, 19-32; helix 3, 43-57; helix 4, 62-68; helix 5, 96-101. The determined secondary structure was broadly well matched to the protein disorder prediction result using prDOS program (Figure 3A).²³ Furthermore, in the prDOS result, the assignment-missing region (residues 81-85) showed the highest scores of disorder probability, supporting our assumption that the region would be flexible.

To obtain further structural information, we also analyzed the chemical shifts of backbone amide protons (δHN s), additionally to the aforementioned backbone ^{13}C chemical shifts. It is generally accepted

that δHN also reflects the secondary structure information; up-field shifts in α -helices, whereas down-field shifts in β -strands, relative to the reference chemical shifts of individual amino acids.²⁴ However, δHN s particularly in α -helices are also sensitive to the structural environments as follows; δHN of the i^{th} residue (δHN^i) is down-field shifted by its strong hydrogen bonds with other residues. In addition, the δHN^i is further down-field shifted by an anisotropy effect of the $i-4^{\text{th}}$ carbonyl group, whereas it is up-field shifted by the anisotropy effects of the $i-3^{\text{th}}$ and $i-2^{\text{th}}$ carbonyl groups.²⁵ Ten residues (18, 19, 30, 36, 48, 61, 64, 67, 68, and 92) in Tid1-eJD appeared with remarkable down-field shift of δHN , of which degree is over the standard deviation value (0.636 ppm) from the mean (8.017 ppm) of all δHN s determined (Figure 3B). Among them, three residues were found in helix 2 and four residues in helix 4. Therefore, it is suggested that the two helices could critically contribute to the structural stability maintaining the overall architecture of helical packing, as such prominent down-field shifts are likely attributed to inter-helix hydrogen bonds.

In summary, we obtained a near complete backbone NMR assignments of the putative p53-binding domain, Tid1-eJD. Based on the chemical shift analysis, five α -helices (four in JD and one in extended region) and a flexible disordered region between the last (C-terminal) two helices were identified. In addition, the second and fourth helices are considered as a central core stabilizing the helical framework. All these results of NMR assignments and structural characterization are expected to constitute the most fundamental and crucial data for the progressing structural investigation of the atomic structure of Tid1-eJD and its molecular interaction with p53 and/or mortalin.

Acknowledgements

This research was supported by Basic Science Research Program through the National Research Foundation of Korea (NRF) funded by the Ministry of Education, Science and Technology (No. 2013R1A1A2007774). The research was also supported in part by the International Science and Business Belt Program through the Ministry

of Science ICT (No. 2017K000490). This study made use of NMR machine at Korea Basic Science Institute (KBSI), Ochang, Korea.

References

1. A. L. Horwich, *Cell* **157**, 285 (2014)
2. F. U. Hartl, A. Bracher, and M. Hayer-Hartl, *Nature* **475**, 324 (2011)
3. M. E. Feder and G. E. Hofmann, *Annu. Rev. Physiol.* **61**, 243 (1999)
4. F. U. Hartl, *Nature* **381**, 571 (1996)
5. J. R. Glover and S. Lindquist, *Cell* **94**, 73 (1998)
6. X. B. Qiu, Y. M. Shao, S. Miao, and L. Wang, *Cell. Mol. Life Sci.* **63**, 2560 (2006)
7. M. E. Cheetham and A. J. Caplan, *Cell Stress Chaperones* **3**, 28 (1998)
8. M. J. Vos, J. Hageman, S. Carra, and H. H. Kampinga, *Biochemistry* **47**, 7001 (2008)
9. H. H. Kampinga, J. Hageman, M. J. Vos, H. Kubota, R. M. Tanguay, E. A. Bruford, M. E. Cheetham, B. Chen, and L. E. Hightower, *Cell Stress Chaperones* **14**, 105 (2009)
10. A. Ahmad, A. Bhattacharya, R. A. McDonald, M. Cordes, B. Ellington, E. B. Bertelsen, and E. R. Zuiderweg, *Proc. Natl. Acad. Sci.* **108**, 18966 (2011)
11. F. Hennessy, W. S. Nicoll, R. Zimmermann, M. E. Cheetham, and G. L. Blatch, *Protein Sci.* **14**, 1697 (2005)
12. P. Bischofberger, W. Han, B. Feifel, H. J. Schonfeld, and P. Christen, *J Biol Chem* **278**, 19044 (2003)
13. B. Lu, N. Garrido, J. N. Spelbrink, and C. K. Suzuki, *J. Biol. Chem.* **281**, 13150 (2006)
14. J. Syken, T. De-Medina, and K. Munger, *Proc. Natl. Acad. Sci.* **96**, 8499 (1999)
15. J. Proft, J. Faraji, J. C. Robbins, F. C. Zucchi, X. Zhao, G. A. Metz, and J. E. Braun, *PLoS One* **6**, e26045 (2011)
16. B. Y. Ahn, D. L. Trinh, L. D. Zajchowski, B. Lee, A. N. Elwi, and S. W. Kim, *Oncogene* **29**, 1155 (2010)
17. D. L. Trinh, A. N. Elwi, and S. W. Kim, *Oncotarget* **1**, 396 (2010)
18. S. Kaul and R. Wadhwa, "Mortalin Biology: Life, Stress and Death" Chap. 14, Springer, New York, 2012
19. S.-H. Lee, D.-W. Sim, E.-H. Kim, J. H. Kim, and H.-S. Won, *J. Korean. Magn. Reson. Soc.* **21**, 50 (2017)
20. H.-S. Won, S. H. Park, H. E. Kim, B. Hyun, M. Kim, and B. J. Lee, *Eur. J. Biochem.* **269**, 4367 (2002)
21. F. Delaglio, S. Grzesiek, G. W. Vuister, G. Zhu, J. Pfeifer, and A. Bax, *J. Biomol. NMR* **6**, 277 (1995)
22. Y. Shen and A. Bax, *J. Biomol. NMR* **56**, 227 (2013)
23. T. Ishida and K. Kinoshita, *Nucleic Acids Res.* **35**, W460 (2007)
24. S. P. Mielke and V. V. Krishnan, *Prog. Nucl. Magn. Reson. Spectrosc.* **54**, 141 (2009)
25. T. Asakura, K. Taoka, M. Demura, and M. P. Williamson, *J. Biomol. NMR* **6**, 227 (1995)